

## Study the Structural and Magnetic Properties of (x) Ni<sub>0.4</sub>Cu<sub>0.2</sub>Zn<sub>0.4</sub> Fe<sub>2</sub>O<sub>4</sub> + (1-x) BaTiO<sub>3</sub> Prepared by Solid State Reaction Method

AmelKhalaf Salem<sup>1</sup>, Adnan Raad Ahmad<sup>2</sup>, Abdul Sami FawziAbdulaziz<sup>3</sup>

<sup>1</sup>Tikrit University - College of Education for Pure Sciences - Department of Physics

<sup>2</sup>Tikrit University- College of Education for Pure Sciences - Department of Physics

<sup>3</sup>University of Tikrit - College of Science - Department of Physics

amalalbaiaty993@st.tu.edu.iq, abdulsamee\_fawzi@tu.edu.iq<sup>3</sup>

**Article History:** Received: 11 January 2021; Revised: 12 February 2021; Accepted: 27 March 2021; Published online: 4 June 2021

**Abstract:** The electrophoretic compounds were prepared with the chemical formula (x) Ni<sub>0.4</sub>Cu<sub>0.2</sub>Zn<sub>0.4</sub> Fe<sub>2</sub>O<sub>4</sub> + (1-x) BaTiO<sub>3</sub>, and with weight ratios (x = 0.15,0.30,0.45), by the solid-state method interactions. The prepared samples were annealed at (9500°C) for a period of (4hr). After that, physical examinations were made to it, as well as studying the structural properties of lattice constants (a, c), grain size (D<sub>p</sub>), density of both types, apparent density (a) and density in terms of x-ray diffraction (x-ray<sub>ρ</sub>), where it was found that it increases with increasing fear phase focus. While the porosity decreases. A scanning electron microscope (SEM) was used to calculate the granular size (D<sub>nn</sub>) and study its homogeneity and its role in improving the physical and magnetic properties. EDAX technology has also been used to confirm component ingredients and weight ratios. The residual magnet (Mr) for all samples was calculated according to (VSM) technique.

### 1. Introduction

The great industrial development that the world is witnessing in all fields is the reason behind the engineers and physicists seeking to make various alternatives to widely used materials in the industry as these alternatives have distinctive specifications and high quality in terms of light weight and mechanical properties, which makes them used in various electronic applications represented by central memory units. And wired, wireless and other devices, and therefore, materials composite) have been used to provide a mixture of properties that cannot be obtained from the constituent materials [1], and composite materials are defined as the result of mixing two or more specific materials to obtain new materials with distinct physical and mechanical properties that differ from The properties of its constituent materials, and that its properties depend on the properties of its components, and the composite material is composed of the matrix, which is either ceramic, metallic, or polymeric, and the material reinforcement, which improves or increases the strength and stiffness of the base material[2].

The composite materials are characterized by the following [3]

- 1- Easy to form complex shapes with large sizes and dimensions.
- 2- Its durability is much greater than that of traditional materials.
- 3- Great resistance against the spread of cracks that occur as a result of vibrations, and thus are excellent as rotational axes.
- 4- It has high thermal resistance.
- 5- Significant light weight without affecting durability properties.

Powder technology has occupied an advanced position in materials science to obtain composite materials, as it allows the use of a wide range of materials such as materials with low melting points and materials with high melting points, as this technology is one of the most important methods used in the fields of industrial production, as well as It provides an acceptable service performance and reduces the economic cost of manufactured parts. [4]

### Practical Part

The research includes the manufacture of ferrite and ferroelectric biphasic compounds with the formula (x) Ni<sub>0.4</sub>Cu<sub>0.2</sub>Zn<sub>0.4</sub> Fe<sub>2</sub>O<sub>4</sub> + (1-x) BaTiO<sub>3</sub> and named N<sub>0</sub>, N<sub>1</sub>, N<sub>2</sub>, N<sub>3</sub>, N<sub>4</sub> using solid state reactions and studying the structural properties, surface topography and magnetic properties of HL in terms of techniques. XRD, SEM, VSM.

### 1-2 Preparing Samples

The solid-state reaction method was used in preparing samples in three stepsThe method of preparing the ferrite phase whose chemical formula is (Ni<sub>0.4</sub>Cu<sub>0.2</sub>Zn<sub>0.4</sub>Fe<sub>2</sub>O<sub>4</sub>), where materials with high purity of not less than 99%

were used, which are nickel oxide (NiO, copper oxide), zinc oxide (ZnO) and iron oxide (Fe<sub>2</sub>O<sub>3</sub>). The weight ratios of the models with a digital scale, by determining the weights depending on the atomic weight of each element, after taking the weight of the required raw materials, they are mixed well with the mediation of (Mortar) and a pestle of agate to be well ground for 3 hr to obtain a homogeneous mixture, then the homogeneous mixture is heated after putting it in Casserole bouquet to 700 ° C for 6hr in an electric oven, after taking it out of the oven, pre-heat again and well for 1hr. After that, sieves with a radius of (0.075µm) were used to obtain fine granules, then the bonding material (PVA) was added at a ratio of (2-3) drop, so that the mixture would hold together during the removal process from the mold, then the samples were compressed under pressure (5 Ton). Finally, the pressed tablets are heated to a temperature of (1000°C for a period of (6hr), and then the samples are gradually cooled until they reach room temperature, in order to obtain the integrated ferrite phase. ), Using high-purity raw materials, which are barium oxide (BaO) and titanium oxide (TiO<sub>2</sub>), and with specific weight ratios, and it was heated at a temperature of 7000C for 12hr to obtain a homogeneous compound. (5Ton), and the pressed tablets are heated to a temperature of (900°C) for a period of (4hr) to obtain an integrated ferroelectric phase.

Or for obtaining the double phases of ferrite - ferroelectric with the chemical formula (Ni<sub>0.4</sub> Cu<sub>0.2</sub> Zn<sub>0.4</sub> Fe<sub>2</sub>O<sub>4</sub> + BaTiO<sub>3</sub>), with different weight ratios for the ferrite phase (X = 0.15,0.30,0.45) and the corresponding ferroelectric compound (X = 0.85, 0.30,0.45), it was manufactured after completing the ferrite and ferrite preparation stages previously mentioned, as weight ratios were taken from the ferrite compound with weight ratios from the ferroelectric compound, and these proportions were mixed and milled for (2 hr) to obtain a homogeneous mixture. After that, (2-3) PVA binders are added and the powder is pressed into a mold of 1cm diameter. After that, they were finally annealed at a temperature of 950 C for a period of (4 hr) so that these prepared samples were ready for study of their structural and magnetic properties.

**2 Scientific Measurements**

**2-2-1 X-ray diffraction (XRD)**

The technique of X-ray diffraction (XRD) is used to study the structural properties of the prepared samples, with respect to the ferrite phase of a cubic crystal structure where the interval distance (d), the lattice constant (a) and the Miller coefficients (hkl) corresponding to each plane in the sample are related to the following mathematical equation [5].

$$d = \frac{a}{\sqrt{h^2 + k^2 + \ell^2}} \dots \dots \dots (1)$$

As for the ferroelectric phase of the quadruple crystal structure, where the lattice constants (a and c) are calculated through the following mathematical relationship. [6]

$$\frac{1}{d^2} = \frac{h^2 + k^2}{a^2} + \frac{\ell^2}{c^2} \dots \dots \dots (2)$$

The crystal size (D<sub>nn</sub>) for all samples was also calculated using the (Debye - Sherrer Equation) [7].

$$D_p = \frac{k\lambda}{\beta \cos\theta} \dots \dots \dots (3)$$

Where is:

K: The formal constant and its value (0.9 )

λ : Wavelength and its value (1.54060Å)

Θ: Brak's angle, after multiplying it by ( $\frac{\pi}{180}$ ), converted from (Degree to (Radian)

β :The width of the top is at the midpoint of the intensity ( FWHM)

As for the density in terms of X-ray diffraction of the frite compounds, it is calculated through the following mathematical relationship [8]

$$\rho_{x_1} = \frac{8M}{Na^3} \dots \dots \dots (4)$$

Whereas:

M: Molecular Weight in (gm), N: Avocado 6.023X10<sup>23</sup>mol<sup>-1</sup> number

For ferroelectric compounds with a quadrangular structure, the X-ray intensity is calculated according to the following mathematical relationship. [9].

$$\rho_{x_2} = \frac{M}{Na^2c} \dots\dots\dots (5)$$

For the ferrite-ferroelectric compounds, the X-ray intensity is calculated according to the following mathematical relationship [10].

$$\rho_{x_3} = \frac{M_1+M_2}{V_1+V_2} \dots\dots\dots (6)$$

$M_1 = (y)$  (Molecular Weight of Frite)  
 $M_2 = (1-y)$  (Molecular Weight of Ferroelectric)

$$V_1 = \frac{M_1}{\rho_{x_1}} \dots\dots\dots (7)$$

$$V_2 = \frac{M_2}{\rho_{x_2}}$$

$y =$ Weight ratio (0.15, 0.30 and 0.45).

As for measuring the physical density of all samples, it was done using the following mathematical relationship. [11]

$$\rho_a = \frac{m}{v} \dots\dots\dots (8)$$

Knowing the values of the X-ray intensity and the apparent density, the porosity of the samples was calculated using the following mathematical relationship. [12]

$$P = \frac{\rho_x - \rho_a}{\rho_x} 100\% \dots\dots\dots (9)$$

Whereas:

$\rho_x$  : density in terms of X-ray diffraction

$\rho_a$  : : bulk density

### 3.Results and Discussion

#### 3.1 X-ray diffraction (XRD)

Figure (1) represents the X-ray diffraction pattern for the double ferrite-ferroelectricphases, with the weight ratios of the ferrite phase (0.0,0.15,0.30,0.45,1) and the equivalent for the ferroelectric phase (1,0.85,0.70,0.55,0.0) and named (N0, N1, N2 , N3, N4) respectively. As it was found from the previous figures that the greatest intensity of X-ray absorption of the ferrite phase and the ferroelectric phase were at the crystalline levels (311) and (110), respectively, while figures N<sub>1</sub>, N<sub>2</sub> and N<sub>3</sub> indicate that the intensity of the ferrite phase increased with its concentration in biphasic. As for table (1), it shows the results of the lattice constants, the density of its two types, and the porosity of the compounds, as there was a slight change in the lattice constants of the samples when compared with the lattice constants in the ferrite and ferroelectric phases separately. While the lattice constant in the ferroelectric phase continues to decrease in the ferroelectric phase (BTO), as for the (c/a) ratio decreased in the BTO phase, it indicates that the crystal structure is frequent in the compound, and also the intensity

of x-rays and the apparent density have decreased for these compounds While the porosity increased if compared with the ferrite and ferroelectric compounds separately [13]

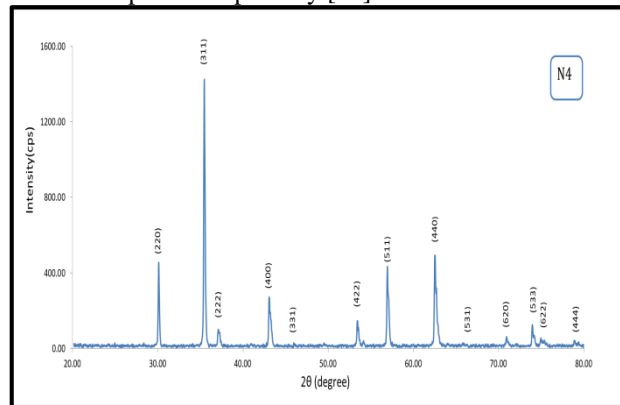
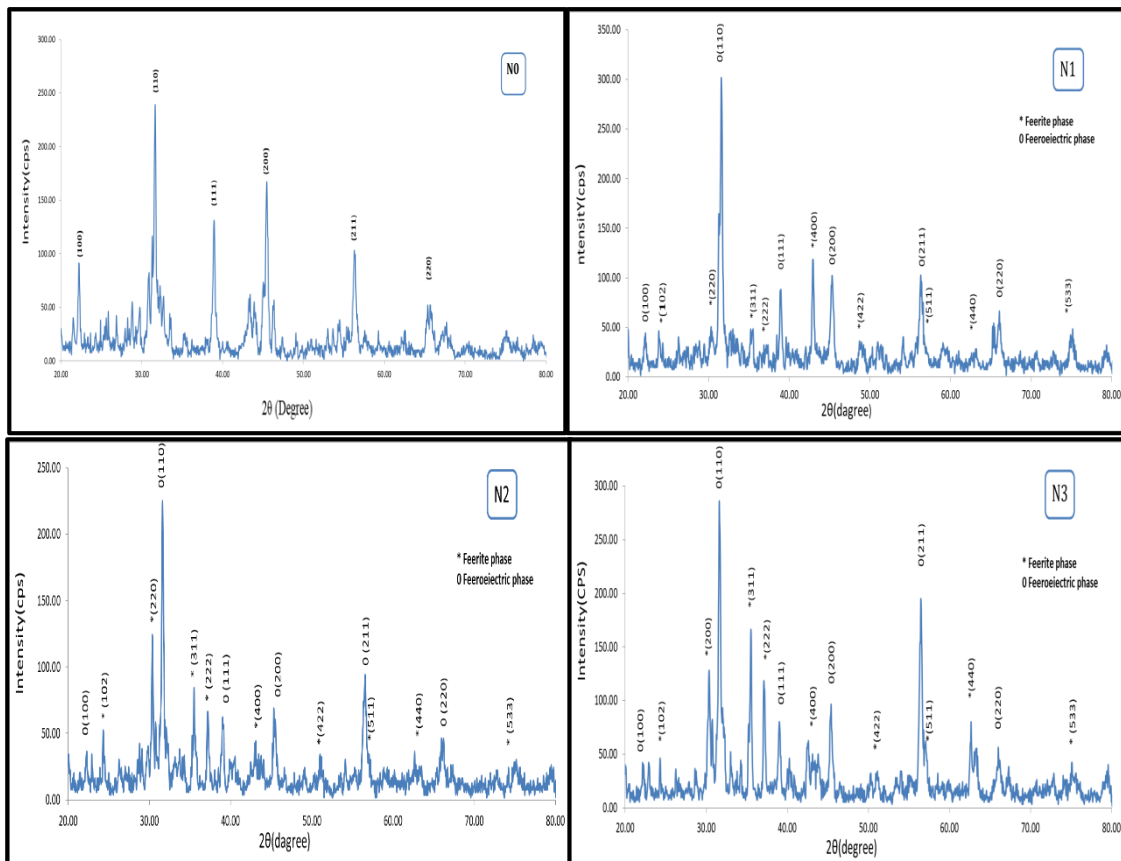


Figure (1) X-ray diffraction patterns of (x) Ni<sub>0.4</sub>Cu<sub>0.2</sub>Zn<sub>0.4</sub> Fe<sub>2</sub>O<sub>4</sub> + (1-x) BaTiO<sub>3</sub>.

Table (1): The lattice constant and density in terms of X-ray diffraction (ρ<sub>X</sub>), physical density (a) and porosity for N<sub>0</sub>, N<sub>1</sub>, N<sub>2</sub>, N<sub>3</sub>, N<sub>4</sub> samples, respectively.



Compo sition (x) Mole%	Lattice parameters of the phases				C.S (nm)	P <sub>x</sub> g/cm <sup>3</sup>	P <sub>a</sub> g/cm <sup>3</sup>	P %
	Ferri te	Ferroelectric						
Sample	a(Å)	a(Å)	c(Å)	c/a				
<b>(x)Ni<sub>0.4</sub>Cu<sub>0.2</sub>Zn<sub>0.4</sub> Fe<sub>2</sub>O<sub>4</sub>+(1-x)BaTiO<sub>3</sub></b>								
N <sub>0</sub>	----- -	3.98 81	4.048 5	1.01 51	36.8	6.013 9	3.1089	48. 30

N <sub>1</sub>	8.364 9	4.00 00	3.991 2	0.99 78	23.117	5.466 91	2.9137	46. 70
N <sub>2</sub>	8.381 1	4.00 00	3.899 8	0.97 49	25.553	5.450 63	3.0318	45. 13
N <sub>3</sub>	8.381 1	3.99 10	3.983 6	0.99 81	26.972	5.441 82	3.0208	44. 79
N <sub>4</sub>	8.381 9	-----	-----	----- -	39.5	5.369 2	3.3558	37. 50

**Table (2): Miller coefficients (hkl) and the interlayer distance (d) that were obtained through the results of X-ray diffraction and interlayer distance technology in the ASTM card for samples with (Standard Card 29-230-0296).**

hkl	d <sub>Std</sub>	dN <sub>0</sub> (Å)	dN <sub>1</sub> (Å)	dN <sub>2</sub> (Å)	dN <sub>3</sub> (Å)	dN <sub>4</sub> (Å)
(100)	4.0029	3.9958	4.0096	3.9866	3.9932	-----
(220)	2.9531	-----	2.9096	2.9395	2.9428	2.5282
(110)	2.8299	2.8251	2.8304	2.8254	2.8245	2.4222
(311)	2.5185	-----	2.5484	2.5260	2.5261	-----
(222)	2.4113	-----	2.4190	2.4154	2.4183	2.0974
(111)	2.3110	2.3117	2.3116	2.3060	2.30637	-----
(400)	2.0884	-----	2.0841	2.0997	2.0979	1.7129
(200)	1.9890	1.9940	1.9999	1.9956	1.9974	-----
(422)	1.7049	-----	1.7256	1.7049	1.7129	1.6152
(211)	1.6341	1.6322	1.6307	1.6283	1.6292	1.4759
(511)	1.6074	-----	1.6160	1.6154	1.6142	-----
(440)	1.4766	-----	1.4825	1.4816	1.4806	1.3332
(220)	1.4151	1.4208	1.4244	1.4158	1.4035	-----
(533)	1.2738	-----	1.2679	1.2777	1.2846	2.5282

**2-3 Scanning Electron Microscopy (SEM)**

Figure (2) states an image of samples N<sub>0</sub>, N<sub>1</sub>, N<sub>2</sub>, N<sub>3</sub>, N<sub>4</sub> using a scanning electronic microscope (SEM) technique. The image showed different shapes, including nano wire and semi-spherical shapes. Table (3) shows

the average grain size of the samples under study as well as making sure of the elementary elements used and their proportions in the manufacture of samples in terms of the EDAX technology attached to the SEM device.

Figure (3) Scanning electronic microscope images (SEM) and (EDAX) for samples N<sub>0</sub>, N<sub>1</sub>, N<sub>2</sub>, N<sub>3</sub>, N<sub>4</sub> respectively.

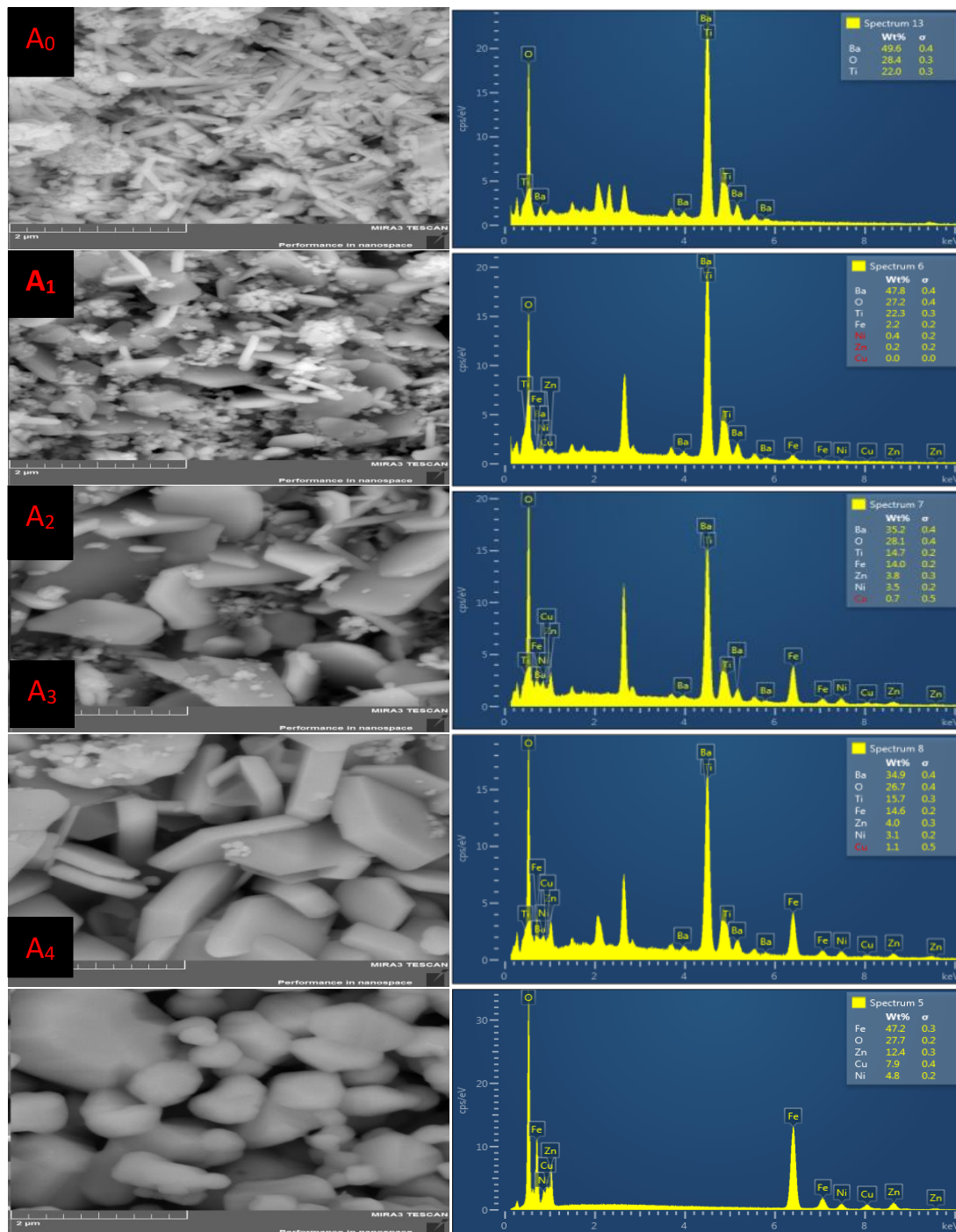


Table [3]: shows the results of the grain size of the samples N<sub>0</sub>, N<sub>1</sub>, N<sub>2</sub>, N<sub>3</sub>, N<sub>4</sub> respectively.

Samples	Grain size (nm)
N <sub>0</sub>	0.30214
N <sub>1</sub>	0.69283
N <sub>2</sub>	0.87757
N <sub>3</sub>	1.04033
N <sub>4</sub>	1.12083

### 3-3 Magnetic Hysteresis

Figure (4) Placing VSM of N<sub>1</sub>, N<sub>2</sub>, N<sub>3</sub>, N<sub>4</sub> samples respectively at room temperature. It was found from the figure that the saturation magnetism (Ms) and the residual magnetism (Mr) increase with the increase in the ferritic content and the reason for this is due to the distribution of Kaiton and Neil Model. Where the (zn<sup>+2</sup>) ion occupies the tetrahedral sites (A-site), while the (Ni<sup>+2</sup>) ion occupies the (B-site) octahedral sites in Freight's AB<sub>2</sub>O<sub>4</sub> spindle structure. And that the (zn<sup>+2</sup>) ion displaces the (Fe<sup>+3</sup>) ion from the A site to the B site, and the result was an increase in the magnetic moment at the B site in the crystal lattice, in addition to an increase in the net magnetic moment of the crystal. Also, in all compounds, the values of the magnetization (Ms) and residual magnetism (Mr) decrease when increasing the ferroelectric phase content (BTO), which is proportional to the decrease in the ferrite phase content of the compound [14].

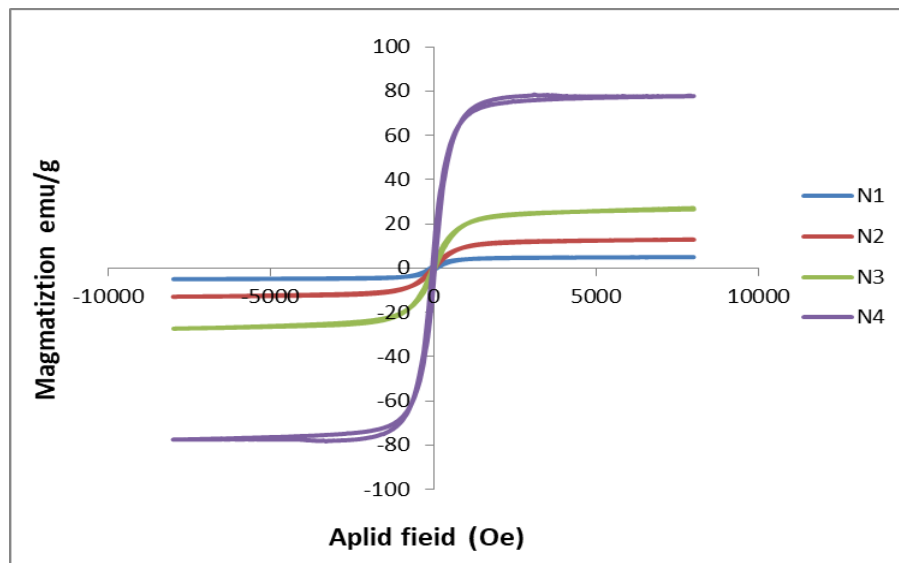


FIG. 4 represents the regurgitation loop for samples N<sub>1</sub>, N<sub>2</sub>, N<sub>3</sub>, N<sub>4</sub>

Table [3] the values of magnetism (Ms) and residual magnetism (Mr) for samples N<sub>1</sub>, N<sub>2</sub>, N<sub>3</sub>, N<sub>4</sub> respectively.

Samples	Ms(emu/g)	Mr(emu/g)
N <sub>1</sub>	5.0226	0.4775
N <sub>2</sub>	12.9201	0.6353
N <sub>3</sub>	27.2088	1.1565
N <sub>4</sub>	77.690	1.2968

### References

- [1]. H.P.Garg, and J.Prakash, "Solar Energy \_ Fundamental & Application", 7threprint, Tata MG Graw-.i Hill Publishing Company Limited, 2006.
2. SilwanBehnamAbd Al-Ahad Al-Sa'aur "Study of the Mechanical Properties of Composite Materials Using Glass Fibers and Kevlar" Master Thesis, Department of Machinery and Equipment, University of Technology, 1998.
3. SalihYunusDarwish "Study of the Physical Properties of a Composite (Basalt: Aluminum) Prepared by the Powder Technology Method" PhD thesis, PhD, Tikrit University, 2018.
4. F.C. Campbell , "Manufacturing Technology for Aerospace Structural Materials ", First edition 2006 Library of Congress
5. M. J. Iqbal, M. N. Ashiq, P. Hernandez-Gomez and J. M. Munoz, "Synthesis, Physical, Magnetic and Electrical Properties of Al-Ga Substituted Co-precipitated Nanocrys- talline Strontium Hexaferrite," Journal of Magnetism and Magnetic Materials, 320 ( 2007) 881- 886.
6. Rajehkumar,Neerajkhare,Vijaykumar,andBhalla,Applied Surface Scince, 7 254 (2008).
7. T.J. Shindea.elt, " DC resistivity of Ni–Zn ferrites prepared by oxalate precipitation method", Materials Chemistry and Physics, 87–91. (2008).
8. Y. S. Hong; M. Ho; Hsu, H. Y. Liu, C. T. J. Magn. Magn. Mater, 279,401, (2004).

9. I.H. Gul, A. Z. Abbasi, F. Amin, M. Anis-ur-Rehman, A. Maqsood, J. Magn. Magn. Matter.311 (2007) 494-499.
10. Devan R. S., Chougule B. K., "Magnetic properties and dielectric behavior in ferrite/ferroelectric particulate composites", *Physical B Condensed Matter* 393 (2007) 161-166.
11. T.C. Paul Barnes, "Simon Jacques Advanced Certificate in Powder Diffraction on the Web. Bragg's Law", (2006).
12. G. I.H. Abbasi, A. Z. Amin, F. Anis-ur-Rehman, M. Maqsood, A., J. Magn. Magn. Matter.311(2007) (494-499),.
13. AtiyaFarheen, ThirupathiGadipelly, "Rajender Singh Multiferroic properties of ferromagnetic and ferroelectric coupled Mn-Zn ferrite-BaTiO<sub>3</sub> composite" 516 (2017) 82-89.
14. P.K. Roy, " Influence of Substitutions and Sintering Aids on Structural and Electromagnetic Properties of NiCuZn Ferrites", Ph.D., National Institute of Technology , (2009) 14-25.